Plasma Processes and Polymers

Direct Plasma Deposition of Lysozyme-Embedded Bio-Composite Thin Films

Fabio Palumbo,* Giuseppe Camporeale, Yi-Wei Yang, Jong-Shinn Wu, Eloisa Sardella, Giorgio Dilecce, Cosima Damiana Calvano, Laura Quintieri, Leonardo Caputo, Federico Baruzzi, Pietro Favia*

Bio-composite coatings, consisting of an organic matrix embedding a bioactive molecule, have been deposited by means of atomizer-assisted atmospheric pressure plasma. Ethylene was chosen as the precursor of the matrix, while the atomizer was fed with a water solution of lysozyme. Coatings chemical composition was investigated by XPS, FTIR and MALDI-TOF spectroscopies, and it has been proved that the one-step inclusion of protein domains in the composite coatings is successful and lysozyme chemical structure is only slightly altered. The amount of embedded lysozyme is as high as 14 μg/cm^2 as evaluated from water release test. Finally, the activity of the plasma-embedded protein is close to that of pure lysozyme as verified against *Micrococcus lysodeikticus* ATCC 4698 through an agar plate diffusion test.

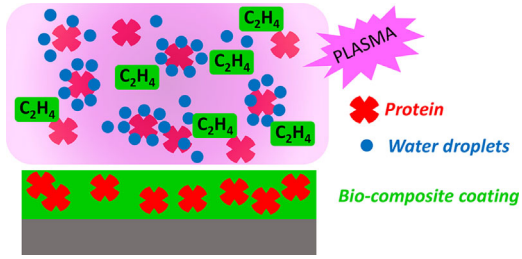

1. Introduction

The synthesis of bio-composite coatings, containing an organic/inorganic synthetic matrix embedding, or grafted with, natural molecules, represents an important technological issue: bio-composite coatings, in fact, bring added value to the material they are deposited on, without affecting its bulk characteristics. This kind of materials is very versatile since, by properly choosing the nature of the matrix and of the coupled biomolecule and their relative amount, the composite properties can be finely tuned, thus matching specific technological requirements in a wide range of applications.

Bio-composite coatings have been developed, for example, by the biosensor industry, with the aim of increasing the selectivity of transistor-based array devices towards specific target biomolecules such as oligo- and poly-nucleotide sequences,[1] saccharides,[2,3] proteins,[4–6] and sometimes cells or viruses.[7–9] In bioreactors, the long-term maintenance and the differentiation of human cells have been improved with the introduction of oligo-peptides at the polymer surface of porous inner membranes.[10] The same strategy has been used to produce antibacterial or cell-growth enhancing coatings either on 3D scaffolds[11,12] or on flat substrates,[13–18] for tissue engineering and regenerative medicine. In food packaging bio-composite coatings have been considered to implement systems prolonging the

F. Palumbo, E. Sardella, G. Dilecce
Institute of Nanotechnology, National Research Council of Italy, Bari, Italy
E-mail: fabio.palumbo@cnr.it
G. Camporeale, C. D. Calvano, P. Favia
Department of Chemistry, University of Bari "Aldo Moro", Bari, Italy
E-mail: pietro.favia@uniba.it
Y.-W. Yang, J.-S. Wu
Department of Mechanical Engineering, National Chiao Tung University, Hsinchu, Taiwan
L. Quintieri, L. Caputo, F. Baruzzi
Institute of Sciences of Food Production, National Research Council of Italy, Bari, Italy

Fabio Palumbo, Giuseppe Camporeale, and Yi-Wei Yang equally contributed to this work.

shelf life of meal, such as fresh cheese.[19] When replacing the biomolecule with synthetic drugs, another use of these coatings can be in drug delivery patches.[20,21]

This wide range of applications has justified a huge research effort aimed to the set-up of versatile straightforward processes for the synthesis of bio-composite films. Photo-polymerization,[22] initiated-Chemical Vapour Deposition (i-CVD),[14] 3D printing,[11] micro-dispensing,[13] many wet chemistry methods[7,12,23,24] can be cited as examples of techniques for bio-composite surface manufacturing. Unfortunately, some drawbacks characterize the above mentioned techniques, limiting their applicability on industrial scale: (i) multi-step processing of substrates or reagents are generally necessary; (ii) potentially harmful solvents and reagents are often required.

Most of these hurdles can be overcome by taking advantage of plasma processes. Literature mostly presents strategies for bio-conjugating active biological compounds (or biologically active ones) to plasma-functionalized substrates. These processes usually include at least two-steps

i) an initial phase, carried out either with low- or with atmospheric-pressure plasma, aimed to enrich the topmost surface of the substrates with functional groups (e.g. grafting oxygen- or nitrogen-containing reactive groups or depositing functionalized films),
ii) the process continues with the adsorption or with the covalent binding of the bioactive molecule to the substrate surface.

The second step is carried out through a wet process; it can consist in the adsorption of the bioactive molecule or in its covalent bond to the substrate surface. Nevertheless, additional reaction steps involving carbodiimides (DIC, EDC or alike) and molecular "spacer" arms (e.g., bis-amine PEG, alkyl diamines, etc.) sometimes are needed to enhance and properly orient the coupling reaction, thus increasing the complexity of the synthesis. This strategy has allowed, for instance, the preparation of anticoagulation,[25,26] antibacterial,[19,27–29] and cell growth enhancing composite coatings[10,15,30] as well as highly selective biosensors for the detection of specific DNA strains or proteins.[3]

Recently, a new one-step strategy for the plasma deposition of bio-composite coatings, based on plasma processing, has been developed: it consists in coupling an atomizer directly to a plasma reactor. This experimental set-up, so far developed mainly for plasma processing at atmospheric-pressure, allows to efficiently spray low vapor pressure pure liquids, salts solutions or even nanoparticles suspensions.[31–36]

In the applications hereby considered, the solution feeding the atomizer can contain the bioactive molecule dispersed in water (or other suitable solvent/buffer solution), and an additional gas/vapor can be added, as a precursor of the matrix. When this complex feed passes through the discharge, the precursor is plasma polymerized forming the matrix, and the biomolecule is incorporated in the plasma polymer during its growth.[31–33] Mild plasma conditions and the formation of a thin watery shell all around the solute during atomization can limit damages of the biomolecule that, consequently, can be embedded in the growing film without loss of structure and activity.[32]

In contrast with the more common two-steps strategy of securing the biomolecule to the substrate surface, this process allows either the retention of the bioactive compound in the coating or its release in the surrounding medium according to the characteristics of the matrix. Moreover, neither enhancers nor spacers are needed.

In the present work, a one-step spray-assisted atmospheric-pressure plasma process for the synthesis of protein carrier systems is presented. The plasma reactor was set in a Dielectric Barrier Discharge (DBD) configuration to allow the deposition of relatively homogeneous films on any kind of thin substrate. Lysozyme (Lyz), an enzyme with antibacterial activity, has been chosen as bio-component of the composite film. Ethylene has been selected as polymerization precursor because it is a simple non-toxic molecule quickly reacting in a plasma environment, leading to the formation of a hydrocarbon matrix. [37] Water was the natural option as solvent for Lyz, and it was chosen because its behavior and interaction with ethylene in atmospheric pressure plasma has been studied and reported in a previous work.[38]

It is important to highlight that preservation of the structure of the embedded biomolecule, once passed through the plasma, is not straightforward. However, in this work, for the first time, at the best of authors' knowledge, the extent of the eventual damages, due to the interaction with the plasma, of the embedded component has been evaluated with a direct chemical approach (MALDI –TOF and HPLC release monitoring).

2. Experimental Section

2.1. Materials

Helium 99.999% and Ethylene 99.95% (Air Liquide) were used as feed gas for the plasma deposition process. Lysozyme from chicken egg white (lyophilized powder, 49 900 U/mg solid, from Sigma–Aldrich, Milan, Italy), was diluted in bi-distilled water at 5 and 8 mg/mL, before experiments. In MALDI-TOF experiments, α-Cyano-4-hydroxycinnamic acid (CHCA), ACTH 18–39 fragment, angiotensin I, renin, insulin β-chain, insulin, cytochrome c, trypsin proteomic grade, dithiothreitol (DTT), iodoacetamide, and ammonium bicarbonate (NH_4HCO_3) were used (Sigma–Aldrich, St. Louis, MO). Water, acetonitrile (ACN), trifluoroacetic acid (TFA) were HPLC grade and were used without further purification. For HPLC release test and lysozyme activity determination, Milli-Q quality (Millipore, Bedford, MA) water was used and chemicals used were of analytical grade unless otherwise stated.

Shards ($24 \times 24\,mm^2$) of 710 μm thick double face polished silicon (100) wafer (MicroChemicals GmbH) were used as substrates for the plasma deposition experiments.

2.2. DBD Reactor Setup

The homemade DBD reactor is schematically shown in Figure 1. It consists of two parallel plates silver electrodes, $8 \times 13\,cm^2$ wide, 5 mm apart, both covered with 0.63 mm thick alumina sheets. The gas inlet is from the shorter side, the feed passes between the electrodes and it is pumped out by an aspirator from the opposite side. The electrodes setup is confined in a sealed Plexiglas chamber.

A Lyz aqueous solution aerosol was generated with an atomizer (mod. 3076, TSI) working with He at a flow rate of 2–5 slm. Since the un-atomized solution was re-circulated and returned in the reservoir of the atomizer, the mass flow rate of the water aerosol was evaluated from the weight difference of the reservoir in each deposition condition. A linear increase of the Lyz solution mass flow rate, in the range 8–136 mg/min, resulted by increasing the atomizer flow rate from 2 to 5 slm. For sake of clarity, being an operative parameter, in the text the results have been reported as a function of the atomizer flow rate. As stated by different authors[33,39] the diameter range of the droplets produced by the atomizer used in the present work in similar conditions is typically submicrometer with an average value around 50 nm.

Ethylene was introduced at 10 sccm and an auxiliary line allowed for the addition of helium to keep its total flow rate at 5 slm. Gas flow rates were controlled by means of electronic mass flow controllers (MKS instruments).

Silicon substrates were placed on the bottom electrode and the chamber was purged with a 5 slm He stream for 5 min. The discharge was ignited using an AC power supply consisting in a function generator (TG1010A, TTi), an amplifier (Industrial Test Equipment Powertron 1 000 A) and a high-voltage transformer (Amp Line). The electrical properties of the plasma were investigated for determining the voltage and the current delivered to the system with a high-voltage (P6015A, Tektronix) and a resistance type current probe, both connected to an oscilloscope (TDS 20145C, Tektronix). The average power was obtained by multiplying the energy per voltage cycle by the frequency; the energy per cycle was calculated from the time integral of the current times the voltage in one cycle. The applied voltage was kept at $6\,kV_{pp}$ at 4 kHz, corresponding to a power value of $0.25\,W\,cm^{-2}$.

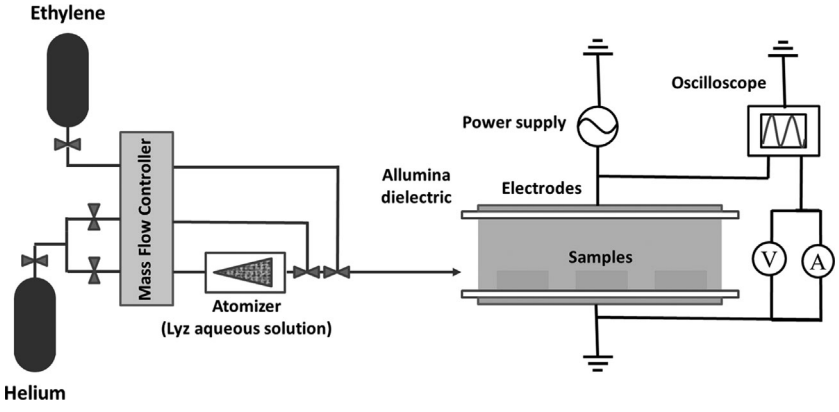

Figure 1. Schematic diagram of aerosol-assisted atmospheric-pressure DBD deposition system.

2.3. Sample Chemical Characterization

X-ray Photoelectron Spectroscopy (XPS) surface characterization of the coatings was performed with a Thermo Fischer Scientific Theta Probe Spectrometer, equipped with monochromatic AlK_α X-rays source (300 μm diameter spot). Survey and high-resolution spectra were acquired at a pass energy of 150 and 100 eV, respectively, in constant analyzer energy (CAE) mode. Charging effects were compensated with a flood gun operating at low electron energy (−1 eV), with extraction potential of 40 V. Calibration of the binding energy (BE) scale was performed by fixing the aliphatic C1s component at BE values of 284.8 ± 0.1 eV. Spectra were manipulated by the software Thermo Avantage (v. 5.24, Thermo Fischer Scientific).

Fourier Transform Infrared Spectroscopy (FT-IR) was carried out to characterize the bulk of the coatings. FT-IR spectra (32 scans, $4\,cm^{-1}$ resolution) were obtained in transmission mode with a Vertex 70V Bruker spectrometer. The spectrometer was evacuated to less than 150 Pa for 5 min before spectrum acquisition, in order to reduce the interference due to atmosphere absorption. Spectra were normalized by the maximum intensity of the CH_3 stretching peak at $2961\,cm^{-1}$. The calculation of the A_{amide}/A_{CHx} absorbtion area ratio, was carried out by a preliminary curve fitting of the $1600–1800\,cm^{-1}$ region. In particular, three contributions with Gaussian shape were considered in that region for the composite coating: at 1 660 (the band corresponding to carbonyl amide group), 1 710 and 1 760 cm^{-1}. Background subtraction, integration of peak areas and any further FTIR spectra manipulation were performed with the Opus 5.0 software (BRUKER Optics).

Mass Spectrometry analysis of the coatings was carried out by means of a Matrix-Assisted Laser Desorption/Ionization Time-Of-Flight (MALDI-TOF) apparatus, Micromass M@LDI - LR (Waters MS Technologies, Manchester, UK) equipped with a nitrogen UV laser (337 nm wavelength), a precision flat target plate sample introduction system bearing a micro-titer target plate, reflectron optics and a fast dual micro-channel plate (MCP) detector. Positive ion spectra were acquired in reflectron mode for peptide mass fingerprinting and in linear mode for protein analysis. The laser-firing rate was 5 Hz, and, unless otherwise specified, 50 laser shots, were used for each well. The resulting spectra were averaged, background subtracted, and smoothed by a Savitzky Golay algorithm in reflectron mode and a mean algorithm in linear mode. A time lag focusing delay of 500 ns was used between the time of the laser pulse and the application of the accelerating voltage.

For protein analysis, 1 μL of the CHCA matrix solution (5 mg/mL in ACN:H_2O 2:1, with 0.1% TFA) was spotted on the silicon slabs, previously stuck on target plate with conductive graphite tape.

To highlight possible protein alterations, consequent to the interaction with the plasma, peptide mass fingerprint was carried out on samples digested with porcine trypsin solution according to Calvano et al.[40] Briefly, an aliquot of each tryptic digest was mixed 1:1 (v/v) with the CHCA solution, and then 1 μL of the sample/matrix solution was spotted, dried, and analysed by MALDI–TOF MS. The raw MS files relevant to tryptic digests have been searched against the non-redundant database Swiss-Prot using MS-Fit server. The search was done against *Gallus gallus* database setting the following modifications: carbamidomethylation of cysteine groups as a fixed modification and oxidation of methionines as a variable modification. Up to three missed cleavages were accepted and a mass tolerance of 0.15 Da was set. Other modifications, such as oxidation of methionine, proline, and tryptophan, likely occurring during plasma processes, were included as well.

2.4. Lysozyme Release Assays

Four replicates of each coated substrate ($20 \times 20\ mm^2$) were put into 12-well Iwaki polystyrene plates with flat base (Sterilin Limited, Newport, UK) and covered with 2 mL of water. Then samples were incubated at 25 °C under gentle stirring (60 rpm). The Lyz amount released from composite films was monitored on 0.05 mL of liquid collected from each well at 0, 15, 30, 45, and 60 min. At the end of incubation, the release solution was removed and analyzed with HPLC or freeze-dried and stored at −20 °C until use for antimicrobial assay. The well and the composite films were further washed with 2 mL of water for 30 min at 25 °C (150 rpm) in order to remove residual Lyz. All liquid samples were analyzed by RP-HPLC with an AKTA Purifier 10 system (GE Healthcare, Uppsala, Sweden) equipped with an UV detector, set at 280 nm. Ten μl of each extract were filtered (0.45 μm, Millipore) and injected into a Zorbax SB-300C 18 reversed-phase column (150×4.6 mm, i.d. 5 μm, 300 Å pore, Agilent, Palo Alto, CA). The separation was carried out using a linear gradient of concentration (v/v) from 20 to 100% of acetonitrile solution containing 0.1% TFA at a flow rate of 1 mL/min for 20 min.

For calibration, aliquots of a Lyz stock solution (5 mg/mL) were diluted in an adequate amount of RP-HPLC mobile phase (final concentration ranged from 1.56 μg/mL to 1 000 μg/mL) and injected in triplicate into the chromatographic system. The analytical detection limit (LOD) and quantification limit (LOQ) of the RP-HPLC method were 2.19 and 7.27 μg/mL, respectively, according to the following equations, where σ is the mean standard deviation and S is the slope of the calibration curve:

$$LOD = 3.3\ \sigma/S \quad LOQ = 10\sigma/S$$

2.5. Agar Diffusion Activity Assay

Freeze-dried samples were suspended in 2 mL of a 0.067 M phosphate buffer (PBS), pH 6.6, containing 22.7 g/L of NaCl and assayed for the antimicrobial activity using the well diffusion lysoplate method[41] with slight modifications. Briefly, 150 mg of freeze-dried intact cells of *Micrococcus lysodeikticus* ATCC 4 698 were dissolved in 5 mL of PBS and incubated at 73 °C for 15 min. Then the cell suspension was kept in an ice bath for about 30 min before being added to 15 mL of melted (46 °C) agar solution (0.7% w/v) and immediately poured in Petri dishes. Wells of 6 mm in diameter were punched out the solidified agar medium and 0.04 mL of solution extracted from the plates was used to fill the agar wells. Petri dishes were immediately incubated overnight at 37 °C. Standard solutions containing 10, 30, and 300 μg/mL of Lyz and PBS were also assayed. Lysozyme activity was calculated measuring the net diameter halos. The halos indicating the antimicrobial activity of the lysozyme solutions from each plate sample were compared with those obtained with the standard solutions. The experiment was repeated three times.

3. Results and Discussion

3.1. Coating Characterization

In Figure 2 the normalized absorption FTIR spectra of films deposited under various atomizer flow rate conditions are reported, together with the corresponding spectrum of pure lysozyme. All deposited coatings exhibit a common hydrocarbon backbone, revealed by the absorption bands relative to CH_2 and CH_3 stretching (3015–2777 cm^{-1}), CH_2 scissoring (1462 cm^{-1}) and C—CH stretching (1383 cm^{-1}). The addition of atomized Lyz solution in the reaction environment led to the appearance of new bands in the spectra due both to the presence of lysozyme and to the reaction of water with the growing film, the latter explained in a previous work.[38] The absorption bands at 1708 and 1056 cm^{-1} can

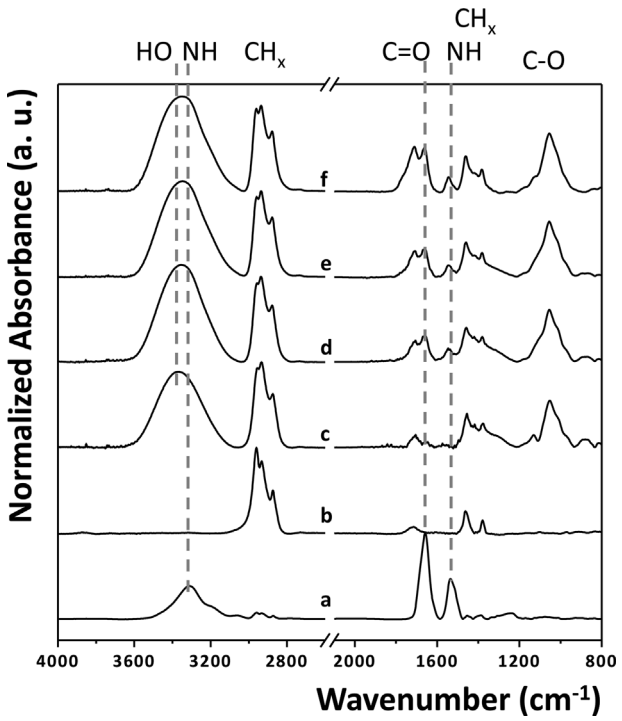

Figure 2. FTIR spectra of: casted Lyz (a); films deposited at an atomizer flow rate of 0 (b), 3 (c), 4 (d), 5 slm (e) with a 5 mg/mL Lyz solution; and at 5 slm atomizer flow rate but with a 8 mg/mL Lyz solution (f).

be attributed to oxygen-containing groups such as C═O and C—O, and not to lysozyme (as well highlighted from the comparison with the protein FTIR spectrum).

Hence, they likely indicate the presence of ketones, aldehydes, ethers, and other oxygen moieties, originating from reaction of the matrix precursor with water. On the other hand the presence of amide bonds (C═O stretch at 1 660 cm^{-1}, and NH bending at 1 537 cm^{-1}) are consistent with the presence of a protein or amino-acid residues embedded in the coating structure. The broad band between 3 640 and 3 022 cm^{-1} is due to the overlap of –OH (broad, typically around 3 400 cm^{-1}) and secondary amide NH (narrower, at 3 310 cm^{-1}, as highlighted in Figure 2a) stretching bands. Such data indicate that the aerosol-assisted deposited coatings can contain lysozyme.

Table 1 shows the relative absorption area of the amide C═O region as a function of the atomizer flow rate. It can be observed that the contribution of the protein related band becomes more important as the lysozyme concentration in the feed increases (i.e., at higher atomizer flow rate and Lyz solution concentration).

The surface chemical composition data of the coatings obtained by XPS are presented in Table 2. Two main observations can be highlighted (i) the oxygen content increases with the flow rate of aerosol, as it can be expected for the introduction of O-containing species (water and Lysozyme), (ii) nitrogen can be revealed only when lysozyme is present in the feed. In fact, the coating deposited when He and ethylene are feeding the plasma without aerosol does not present nitrogen, as well as coatings deposited in very similar conditions by addition of pure water aerosol (hence, lysozyme-free) described in a previous work.[38] These outcomes confirm that nitrogen found in the coatings cannot be ascribed to uptake from the atmosphere or from eventual N_2 contamination present in the reactor and participating at the process. Furthermore, when the atomizer flow rate is raised, the O/C and N/C surface ratios appreciably increase, in agreement with the FTIR results. Since XPS explores a thickness lower than 10 nm, the detection of nitrogen indicates that the protein is present also in the topmost layer of the coating.

However, FTIR and XPS spectroscopies do not allow speculating on the integrity of the embedded protein: the nitrogen and oxygen containing functional groups, revealed both by XPS and FTIR, could be attributed to lysozyme as well as to its fragments, potentially formed in the plasma. MALDI-TOF-MS analysis allows for detection and identification of intact macromolecular species such as proteins; for this reason, drop-casted native lysozyme and plasma deposited Lyz containing coatings, obtained from a 8 mg/mL Lyz solution atomized at 5 slm (hereafter indicated as HiLyz), have been analyzed. As negative control, coatings deposited in the same plasma conditions from Lyz-free water aerosol have been analyzed as well.

The MALDI spectra of native Lyz (Figure 3a) and of the Lyz-embedded plasma deposited coating (Figure 3b) clearly

Table 1. Relative area intensity ratio of the amide band at 1660 cm^{-1}, A_{amide}/A_{CHx} with respect to the CH_x stretching absorption, at different atomizer flow rate and Lyz solution concentration.

Atomizer flow rate (slm)	$[Lyz]_{atomizer}$ (mg/mL)	$A_{amide\ CO}/A_{CHx}$
0	5	0
3	5	0.03
4	5	0.16
5	5	0.16
5	8	0.26

Table 2. XPS atomic concentration for lysozyme containing coatings deposited at different atomizer flow rates.

Atomizer flow rate (slm)	C1s (%)	O1s (%)	N1s (%)
0.0	93.8	6.2	0
3.0	82.5	17.2	0.3
4.0	76.6	22.0	1.4
5.0	76.4	22.0	1.6

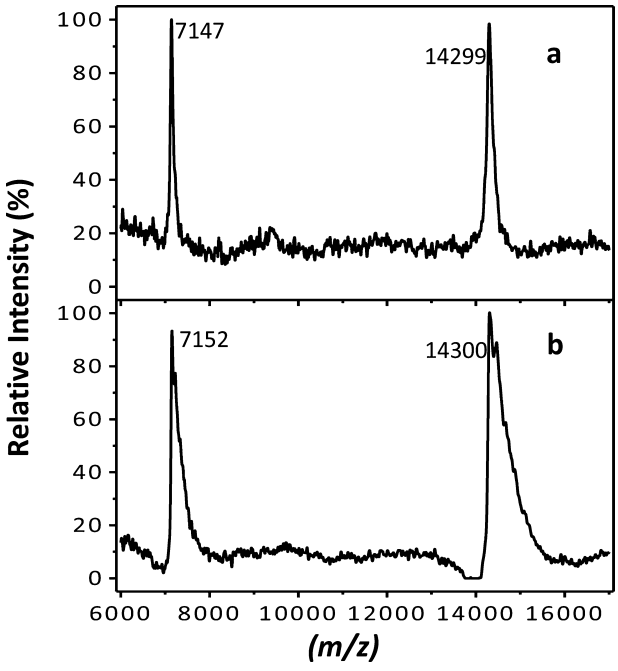

Figure 3. MALDI-TOF mass spectra of native lysozyme (a) and the HiLyz sample (b).

shows the mono- and bi-charged ions of lysozyme at m/z 14 300 and 7 150, respectively (mass accuracy of 100 ppm), indicating that the protein is still intact in the coating after the plasma process. The analysis at lower masses confirmed the absence of smaller peptides. The occurrence of the intense multiple charges ion (i.e., $M+2H^+$), favored by CHCA,[42] enables a more accurate mass determination because the resolution is higher at lower mass over charge, m/z, ratio. However, the spectrum of the Lyz composite coating presents broader peaks, probably due to some degradation reactions or dehydration/oxidation processes in the plasma phase. The lysozyme-free coating leads to a featureless MS spectrum (not shown).

With the aim to get more insights into the structures and sites of the modifications, native protein and Lyz-embedded samples have been enzymatically digested before MS analysis. Figure 4 reports the MALDI mass spectra acquired on drop-casted lysozyme (Figure 4a) and on plasma-deposited Lyz-containing coating (Figure 4b), with CHCA as matrix.

The observed m/z values have been confidently identified after database search as tryptic peptides of lysozyme with sequence coverages of 80.3% and 83.0% for native Lyz and the plasma deposited one, respectively. The spectra showed a similar profile with the same major ions attributable to peptides arising from lysozyme. However, a closer examination of the spectra revealed some differences as the appearance of new signals for the Lyz composite coating. For instance, the m/z ion 1 009.45, observed only in the latter, could correspond to oxidation of tryptophan (80 or 81) of the native peptide at m/z 993.47,

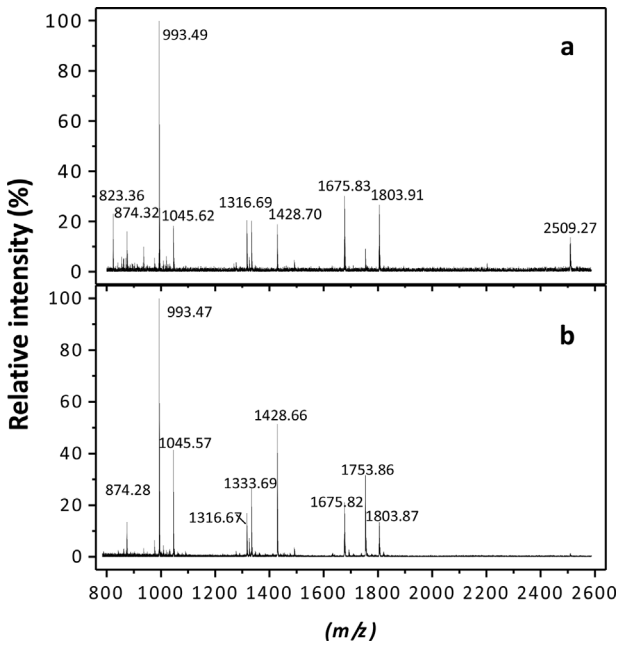

Figure 4. MALDI-TOF mass spectra of native lysozyme (a) and of the HiLyz sample (b) after digestion in tryptic solution.

detected in both samples. Likewise, the peaks at m/z 1 061.57, 1 691.83, 1 819.88, detected only in the plasma deposited coating, could be attributed to peptides with an oxidized methionine or tryptophan.[43] MALDI-TOF-MS has been already used, though rarely,[44,45] in the characterization of plasma polymerized films and, at least in one case, of the plasma deposition of a composite coating containing a drug.[46] However at the best of authors' knowledge, it is the first time that this chemical characterization is carried out for plasma embedded proteins. In particular, in the present work, MS analysis highlights that, though most of the lysozyme is unaltered, some aminoacid residues, the most susceptible, methionine or tryptophan, are oxidized at some extent. This moderate, but significant, modification of the protein, leads to the supposition that it can react with oxidizing species (e.g., oxygen radicals) in the reactive plasma environment.

The deposition rate of lysozyme containing coatings has been measured as a function of the atomizer flow rate. As reported in Table 3, it can be observed that the growth rate strongly depends on the atomizer flow rate, in particular it passes from 20 nm/min to values as high as 75 nm/min, when 5 slm of He is fed through the atomizer. When the protein concentration in the feed solution is increased from 5 to 8 mg/mL (HiLyz sample), the growth rate drops to 43 nm min^{-1}, probably due to quenching of the active species, as a consequence of the increased amount of protein in the plasma.

3.2. Lysozyme Release

To study the behavior of lysozyme-rich composite coatings in aqueous environment, samples have been immersed in distilled water and were analyzed afterwards by means of a profilometer and FTIR absorption spectroscopy. In addition, the lysozyme release in water was investigated more deeply by RP-HPLC.

In Figure 5 the FTIR absorption spectra of films before and after immersion in water for 1 day are reported, the spectrum of native lysozyme is reported as reference. An intensity decrease in the OH/NH stretching broad band can

Table 3. Film deposition rate at different atomizer flow rate and Lyz solution concentration.

Atomizer flow rate (slm)	$[Lyz]_{atomizer}$ (mg/mL)	Deposition rate (nm/min)
0	5	22 ± 2
3	5	45 ± 3
4	5	53 ± 7
5	5	75 ± 8
5	8	43 ± 9

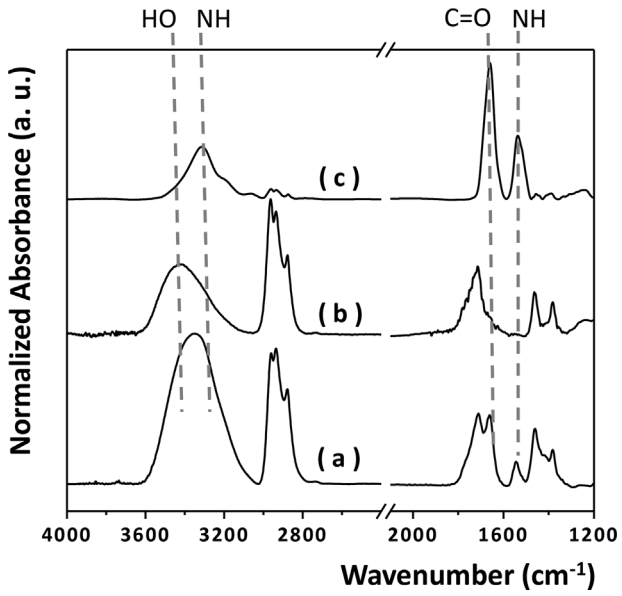

Figure 5. FTIR spectra of the plasma deposited HiLyz coating before (a), and after (b), one-day water immersion, compared to casted Lyz (c).

be observed after 1 day immersion, as well as the shift of the peak toward higher wave numbers, revealing the loss in the amide contribution. This clue, together with the unambiguous decrease of the amide C=O stretching and NH bending bands, leads to conclude that almost all embedded Lyz is released in the surrounding solution within the first day of immersion. Furthermore, after immersion in distilled water for 1 day, the HiLyz sample has shown a thickness decrease from about 800 to 500 nm. Immersion for longer time, 7 days, has not induced further changes in the thickness. This is consistent with the release of unbound protein, evidenced by the FTIR spectra reported in Figure 5, though contribution of eventual loss of loosely bound portion of the matrix cannot be ruled out.

The HPLC analysis results of the release for the coating deposited at an atomizer He flow rate of 5 slm, (with 8 mg/mL Lyz solution), are reported in Table 4. In the initial 15 min of soaking, the lysozyme-containing film has lost most of the total enzyme content. After, the release rate decreased and a concentration of 28 μg/mL is reached in 1 h of incubation. No more changes in protein concentration could be revealed at longer incubation time. Moreover, since the release test has been carried out in 2 mL of water, it could be concluded that the maximum amount of lysozyme that can be released from the coating in water is about 56 μg, leading to a sample surface density of 14 μg/cm^2. Additional washing carried out for 30 min at high stirring speed confirmed the absence of any additional release. It can be estimated that, for the coating hereby presented, about 72% of the lysozyme embedded is released within the first 15 min in water. It is difficult to compare the surface protein density obtained with this

Table 4. Lyz concentration detected in the release solution, for the plasma deposited Hi Lyz coating.

Immersion time [min]	Concentration of Lyz [μg/mL]
0	0
15	20 ± 1
30	23 ± 2
45	25 ± 1
60	28 ± 1

Analyses performed in quadruplicate. Values are average ± standard deviation.

method with others carried out to prepare similar lysozyme-containing coatings However, processes producing lysozyme bonded to plasma functionalized surface[47,48] typically lead to values lower than 2 μg/cm^2. On the other hand, wet methods based on LBL can achieve lysozyme density comparable or slightly higher than the one obtained in this work.[49]

In Figure 6 the chromatogram of the release solution is reported, both for the Lyz-containing coating (Figure 6a), and for a protein free plasma deposited one (Figure 6b). The chromatogram of the solution obtained from the Lyz composite coating presents only one signal at the same elution time of the native protein. No protein fractions could be detected by HPLC, confirming MALDI-TOF data about the absence of main Lyz alterations (e.g., fragmentation in smaller fragments/peptides) in the plasma deposited coatings. MALDI-TOF outcomes seem to be also confirmed by the lysozyme peak shown in Figure 6a, that

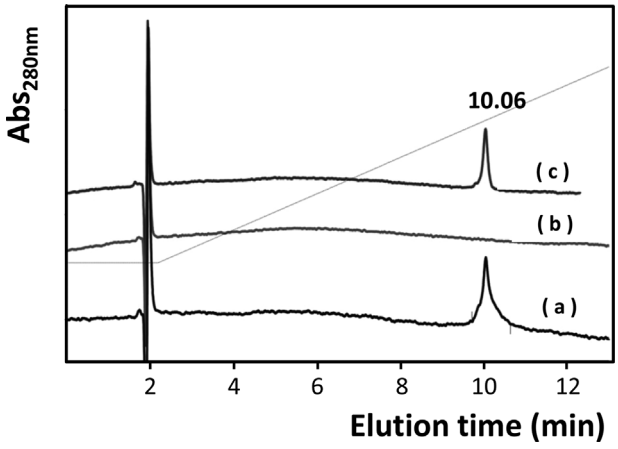

Figure 6. Reverse Phase Chromatogram of solutions sampled after 60 min of extraction from the HiLyz coating (a), and from the coating plasma deposited in the same condition without lysozyme (b). Track (c) refers to the native protein.

Table 5. Agar diffusion activity test results for the HiLyz coating.

Well content	Inhibition halo diameter [mm]
C_2H_4/Lyz_{sol} HiLyz coating	8 ± 1
C_2H_4/H_2O plasma deposited coating (control)	0
Lyz standard solution (10 μg/mL)	0
Lyz standard solution (30 μg/mL)	6 ± 1
Lyz standard solution (300 μg/mL)	12 ± 1
Blank (negative control)	0

is anyway wider compared to the reference (Figure 6c), leading to suppose that some limited modification, such as oxidation or hydroxylation, took place on single Lyz amino-acids. No protein was found released from the negative control coating (Figure 6b)

3.3. Agar Diffusion Assay

In order to verify if Lyz released by plates retained its biological activity once plasma processed to form a composite coating, an agar test against *Micrococcus lisodeikticus* was performed. Since the addition of 150 mg *M. lysodeikticus* cells confers opalescence to a solidified agar solution (0.7% w/v), when active lysozyme diffuse through porous agar, it disrupts bacterial cell walls, turning agar transparent and creating halos all around the wells. Lysis net halos diameters are reported in Table 5. For the solution released from the plasma deposited Lyz coating, an halo with a diameter of about 8 mm has been estimated, which is quite close to the one from a 30 μg/mL native protein solution, in agreement with the concentration of lysozyme found in plate extracts evaluated by RP-HPLC analysis. As expected, no lysis halos were found for solutions obtained from protein-free coatings.

It can then be concluded that the agar lysis test confirms that the plasma-trapped enzyme, despite the slight modifications underwent in the plasma phase (as highlighted by HPLC and MS investigations), keeps most of the biological activity.

4. Conclusions

To summarize, thin lysozyme-containing hydrocarbon coatings have been deposited by means of aerosol assisted atmospheric pressure plasmas in a one-step process. The embedding process has been demonstrated by XPS, FTIR, and MALDI-TOF spectrometry. The latter, in particular, being a suitable method for detecting biological macromolecules, from one side confirmed the presence of intact lysozyme, on the other hand it was able to detect limited region of the protein likely oxidized by the plasma during the process.

The release of the protein into water has been verified; the presence of lysozyme has been furtherly confirmed, as well as its release from the coating. This property makes the bioactive coatings appealing for fast drug delivery systems. In fact, notwithstanding the alterations of the protein detected by MALDI-TOF, the biological activity of the embedded lysozyme is kept, as assessed by the agar diffusion test.

Such results demonstrate the possibility to successfully include active enzymes, and bio-active molecules at large, in plasma-polymerized polymeric coatings, using a one-step procedure, even though stability studies should be evaluated over longer time periods.

Since the bio-activity seems to be retained, important perspective applications open up leading to various applications such as dry manufacturing of drug carrier systems with modulated delivery behavior.

Acknowledgments: The authors show gratitude to the National Science Council (Taiwan) for the grant support 102-2917-I-009-030 to Y.-W. Yang. The projects LIPP (Rete di Laboratorio 51, Regione Puglia), SISTEMA (PON MIUR) and RINOVATIS (PON, MIUR) are gratefully acknowledged for funding. This research is included in the EC COST action MP1101 "Biomedical Applications of Atmospheric Pressure Plasma Technology". Mr. Savino Cosmai (IMIP-CNR) and Mr. Danilo Benedetti (University of Bari) are acknowledged for their valuable technical assistance.

Received: March 5, 2015; Revised: May 1, 2015; Accepted: May 14, 2015; DOI: 10.1002/ppap.201500039

Keywords: aerosol assisted plasma; bio-composite coating; dielectric barrier discharges; lysozyme; matrix-assisted laser desorption/ionization mass spectrometry

[1] H. Miyachi, K. Ikebukuro, K. Yano, H. Aburatani, I. Karube, *Biosens. Bioelectron.* **2004**, *20*, 184.
[2] H. Muguruma, A. Hiratsuka, I. Karube, *Anal. Chem.* **2000**, *72*, 2671.
[3] K. Yoshimura, K. Hozumi, *Microchem. J.* **1996**, *53*, 207.
[4] K. Kojima, A. Hiratsuka, H. Suzuki, K. Yano, K. Ikebukuro, I. Karube, *Anal. Chem.* **2003**, *75*, 1116.
[5] M. Magliulo, A. Mallardi, M. Y. Mulla, S. Cotrone, B. R. Pistillo, P. Favia, I. Vikholm-Lundin, G. Palazzo, L. Torsi, *Adv. Mater.* **2013**, *25*, 2090.
[6] P. Lisboa, M.-B. Villiers, C. Brakha, P. N. Marche, A. Valsesia, P. Colpo, F. Rossi, *Micro Nanosyst.* **2011**, *3*, 83.

[7] F. Patolsky, G. Zheng, O. Hayden, M. Lakadamyali, X. Zhuang, C. M. Lieber, *Proc. Natl. Acad. Sci. U. S. A.* **2004**, *101*, 14017.
[8] C. Mao, A. Liu, B. Cao, *Angew. Chem. Int. Ed.* **2009**, *48*, 6790.
[9] E. Uttenthaler, M. Schräml, J. Mandel, S. Drost, *Biosens. Bioelectron.* **2001**, *16*, 735.
[10] L. De Bartolo, S. Morelli, A. Piscioneri, L. C. Lopez, P. Favia, R. d' Agostino, E. Drioli, *Biomol. Eng.* **2007**, *24*, 23.
[11] M. Kim, W.-K. Jung, G. Kim, *Bioprocess Biosyst. Eng.* **2013**, *36*, 1725.
[12] J. Ryu, S. H. Ku, H. Lee, C. B. Park, *Adv. Funct. Mater.* **2010**, *20*, 2132.
[13] J. Sun, E. S. Thian, J. Y. H. Fuh, L. Chang, G. S. Hong, W. Wang, B. Y. Tay, Y. S. Wong, *Microsyst. Technol.* **2012**, *18*, 2041.
[14] M.-J. Kim, B. Lee, K. Yang, J. Park, S. Jeon, S. H. Um, D.-I. Kim, S. G. Im, S.-W. Cho, *Biomaterials* **2013**, *34*, 7236.
[15] L. C. Lopez, R. Gristina, G. Ceccone, F. Rossi, P. Favia, R. d' Agostino, *Surf. Coat. Technol.* **2005**, *200*, 1000.
[16] K. Yoshimura, A. Sakai, T. Horita, K. Hozumi, *Polym. J.* **1996**, *28*, 284.
[17] O. Etienne, C. Picart, C. Taddei, Y. Haikel, J. L. Dimarcq, P. Schaaf, J. C. Voegel, J. A. Ogier, C. Egles, *Antimicrob. Agents Chemother.* **2004**, *48*, 3662.
[18] A. Guyomard, E. Dé, T. Jouenne, J.-J. Malandain, G. Muller, K. Glinel, *Adv. Funct. Mater.* **2008**, *18*, 758.
[19] L. Quintieri, B. R. Pistillo, L. Caputo, P. Favia, F. Baruzzi, *Innov. Food Sci. Emerg. Technol.* **2013**, *20*, 215.
[20] D. M. Panchaxari, S. Pampana, T. Pal, B. Devabhaktuni, A. K. Aravapalli, *DARU J. Pharm. Sci.* **2013**, *21*, 6.
[21] J. I. Lim, W.-K. Lee, *J. Porous Mater.* **2014**, *21*, 783.
[22] H. He, X. Cao, L. J. Lee, *J. Control. Release* **2004**, *95*, 391.
[23] Z. Zhang, F. He, R. Zhuo, *J. Mol. Catal. B Enzym.* **2013**, *94*, 129.
[24] J. Ji, H. Zhu, J. Shen, *Biomaterials* **2004**, *25*, 1859.
[25] P. Favia, F. Palumbo, R. d' Agostino, S. Lamponi, A. Magnani, R. Barbucci, *Plasmas Polym.* **1998**, *3*, 77.
[26] M. Kastellorizios, G. P. A. K. Michanetzis, B. R. Pistillo, S. Mourtas, P. Klepetsanis, P. Favia, E. Sardella, R. d' Agostino, Y. F. Missirlis, S. G. Antimisiaris, *Int. J. Pharm.* **2012**, *432*, 91.
[27] R. Mauchauffé, M. Moreno-Couranjou, N. D. Boscher, C. V. D. Weerdt, A.-S. Duwez, P. Choquet, *J. Mater. Chem. B* **2014**, *2*, 5168.
[28] D. Duday, C. Vreuls, M. Moreno, G. Frache, N. D. Boscher, G. Zocchi, C. Archambeau, C. Van De Weerdt, J. Martial, P. Choquet, *Surf. Coat. Technol.* **2013**, *218*, 152.
[29] G. Chen, M. Zhou, Z. Zhang, G. Lv, S. Massey, W. Smith, M. Tatoulian, *Plasma Process. Polym.* **2011**, *8*, 701.
[30] C. Baquey, F. Palumbo, M. C. Porte-Durrieu, G. Legeay, A. Tressaud, R. d' Agostino, *Nucl. Instrum. Methods Phys. Res. Sect. B Beam Interact. Mater. At.* **1999**, *151*, 255.
[31] P. Heyse, M. B. J. Roeffaers, S. Paulussen, J. Hofkens, P. A. Jacobs, B. F. Sels, *Plasma Process. Polym.* **2008**, *5*, 186.
[32] P. Heyse, A. Van Hoeck, M. B. J. Roeffaers, J.-P. Raffin, A. Steinbüchel, T. Stöveken, J. Lammertyn, P. Verboven, P. A. Jacobs, J. Hofkens, S. Paulussen, B. F. Sels, *Plasma Process. Polym.* **2011**, *8*, 965.
[33] G. Da Ponte, E. Sardella, F. Fanelli, S. Paulussen, P. Favia, *Plasma Process. Polym.* **2014**, *11*, 345.
[34] L.-A. O'Hare, L. O'Neill, A. J. Goodwin, *Surf. Interface Anal.* **2006**, *38*, 1519.
[35] J. Bardon, J. Bour, D. Del Frari, C. Arnoult, D. Ruch, *Plasma Process. Polym.* **2009**, *6*, S655.
[36] F. Fanelli, A. M. Mastrangelo, F. Fracassi, *Langmuir* **2014**, *30*, 857.
[37] P. Heyse, R. Dams, S. Paulussen, K. Houthoofd, K. Janssen, P. A. Jacobs, B. F. Sels, *Plasma Process. Polym.* **2007**, *4*, 145.
[38] Y.-W. Yang, G. Camporeale, E. Sardella, G. Dilecce, J.-S. Wu, F. Palumbo, P. Favia, *Plasma Process. Polym.* **2014**.
[39] W. Somers, M. F. Dubreuil, E. C. Neyts, D. Vangeneugden, A. Bogaerts, *Plasma Process. Polym.* **2014**, *11*, 678.
[40] C. D. Calvano, C. De Ceglie, A. Monopoli, C. G. Zambonin, *J. Mass Spectrom.* **2012**, *47*, 1141.
[41] O. Lie, M. Syed, H. Solbu, *Acta Vet. Scand.* **1986**, *27*, 23.
[42] Z. Liu, K. L. Schey, *J. Am. Soc. Mass Spectrom.* **2005**, *16*, 482.
[43] E. Shacter, *Drug Metab. Rev.* **2000**, *32*, 307.
[44] G. Mertz, T. Fouquet, C. Becker, F. Ziarelli, D. Ruch, *Plasma Process. Polym.* **2014**, *11*, 728.
[45] M. Moreno-Couranjou, F. Palumbo, E. Sardella, G. Frache, P. Favia, P. Choquet, *Plasma Process. Polym.* **2014**, *11*, 816.
[46] C. Amorosi, V. Ball, J. Bour, P. Bertani, V. Toniazzo, D. Ruch, L. Averous, M. Michel, *Mater. Sci. Eng. C* **2012**, *32*, 2103.
[47] D. Puleo, R. Kissling, M.-S. Sheu, *Biomaterials* **2002**, *23*, 2079.
[48] M. Minier, M. Salmain, N. Yacoubi, L. Barbes, C. Méthivier, S. Zanna, C.-M. Pradier, *Langmuir* **2005**, *21*, 5957.
[49] V. A. Izumrudov, E. Kharlampieva, S. A. Sukhishvili, *Biomacromolecules* **2005**, *6*, 1782.